Controls on leaf water hydrogen and oxygen isotopes: A local investigation across seasons and altitude

Jinzhao Liu[a, b*], Chong Jiang[a], Huawu Wu[c], Li Guo[d], Haiwei Zhang[e], Ying Zhao[f]

[a] State Key Laboratory of Loess and Quaternary Geology, Center for Excellence in Quaternary Science and Global Change, Institute of Earth Environment, Chinese Academy of Sciences, Xi'an 710061, China

[b] National Observation and Research Station of Earth Critical Zone on the Loess Plateau of Shaanxi, Xi'an, 710061, China

[c] Key Laboratory of Watershed Geographic Sciences, Nanjing Institute of Geography and Limnology, Chinese Academy of Sciences, Nanjing 210008, China

[d] State Key Laboratory of Hydraulics and Mountain River Engineering & College of Water Resource and Hydropower, Sichuan University, 610065, Chengdu, China

[e] Institute of Global Environmental Change, Xi'an Jiaotong University, Xi'an, 710054, China

[f] College of resources and environmental engineering, Ludong University, 264025, Yantai, China

[*]Corresponding author's email: liujinzhao@ieecas.cn (J. Liu)

Abstract

The stable oxygen ($\delta^{18}O_{leaf}$) and hydrogen ($\delta^{2}H_{leaf}$) isotopes of leaf water act as a bridge

that connects the hydroclimate to plant-derived organic matter. However, it remains unclear whether the source water (i.e., twig water, soil water, and precipitation) or meteorological parameters (i.e., temperature, relative humidity, and precipitation) are the dominant controls on $\delta^{18}O_{leaf}$ and $\delta^{2}H_{leaf}$. Here, we reported a seasonal analysis of $\delta^{18}O_{leaf}$ and $\delta^{2}H_{leaf}$ together with isotopes from potential source waters and meteorological parameters along an elevation transect on the Chinese Loess Plateau. We found that $\delta^{2}H_{leaf}$ values were more closely correlated with source water isotopes than $\delta^{18}O_{leaf}$ values, whereas $\delta^{18}O_{leaf}$ and $\delta^{2}H_{leaf}$ values were similarly correlated with meteorological parameters along the elevation transect. Dual-isotope analysis showed that the $\delta^{18}O_{leaf}$ and $\delta^{2}H_{leaf}$ values were closely associated because of their similar altitudinal and seasonal responses, generating a well-defined isotope line relative to the local meteoric water line (LMWL). We also compared the measured $\delta^{18}O_{leaf}$ and $\delta^{2}H_{leaf}$ values with predicted values by the Craig-Gordon model and found no significant differences between them. We demonstrate that the first-order control on $\delta^{18}O_{leaf}$ and $\delta^{2}H_{leaf}$ values was the source water, and the second-order control was the enrichment associated with biochemical and environmental factors on the Loess Plateau.

Short Summary

What controls leaf water isotopes? We answered the question from two perspectives: respective and dual isotopes. On the one hand, the $\delta^{18}O$ and $\delta^{2}H$ values of leaf water responded to isotopes of potential source water (i.e., twig water, soil water, and precipitation) and meteorological parameters (i.e., temperature, RH, and precipitation)

differently. On the other hand, dual $\delta^{18}O$ and $\delta^{2}H$ values of leaf water yielded a significant linear relationship associated with altitude and seasonality.

Keywords: Leaf water, stable isotope, controls, seasonality, altitude

1 Introduction

The stable isotope compositions of oxygen and hydrogen ($\delta^{18}O$ and $\delta^{2}H$, respectively) are increasingly being used as powerful tracers to follow the path of water from its input as precipitation, movement through the soil, and ultimately to its release as soil evaporation and leaf transpiration (Penna and Meerveld, 2019). Leaf water transpiration plays a key role in regulating the water balance at scales ranging from catchment to global. Terrestrial plants can enrich heavier isotopes (^{2}H and ^{18}O) in leaf water via evaporative fractionation through the stoma (Helliker and Ehleinger, 2000; Liu et al., 2015; Cernusak et al., 2016), which is highly dependent on atmospheric conditions (e.g., temperature and relative humidity) and biophysiological processes (Farquhar et al., 2007; Kahmen et al., 2011; Cernusak et al., 2016). Subsequently, the isotopic signals from leaf water are integrated into plant organic matter, such as cellulose (e.g., Barbour, 2007; Lehman et al., 2017) and leaf wax (Liu et al., 2016, 2021), as powerful proxies used for paleoclimate reconstruction (Pagani et al., 2006; Schefuβ et al., 2011; Hepp et al., 2020). However, although leaf water isotopes are the fundamental parameters in ecohydrology and organic biosynthesis, an adequate understanding of controls of leaf water isotopes and the role of source water and hydroclimate in determining leaf water

isotopes is still lacking.

$\delta^{18}O_{leaf}$ and $\delta^{2}H_{leaf}$ values are influenced first by a plant's source water (mainly water taken up by roots from the soil; Cernusak et al., 2016; Barbour et al., 2017; Munksgaard et al., 2017; Liu et al., 2022), and second by the enrichment associated with transpiration (Munksgaard et al., 2017). Soil water for terrestrial plants generally originates from local precipitation, and precipitation isotopes vary spatially and temporally, being subject to controls including temperature, altitude, latitude, distance from the coast, and amount of precipitation (Bowen, 2010; Bowen and Good, 2015; Cernusak et al., 2016). More specifically, soil water isotopes are determined by a mixture of individual precipitation events with distinct isotopic signals and are also affected by evaporation, both of which lead to the development of isotopic gradients in soil water with depth (Allison et al., 1983; Liu et al., 2015). Many studies have shown that the $\delta^{18}O$ and $\delta^{2}H$ values of root/xylem water can be used to characterize the water sources used by plants (Rothfuss and Javaux, 2017; Wu et al., 2018; Wang et al., 2019; Amin et al., 2020; Zhao et al., 2020; Liu et al., 2021a). These studies rested substantially on the assumption that no isotopic fractionation of $\delta^{18}O$ and $\delta^{2}H$ values occurs during water uptake by plant roots (Dawson and Ehleringer, 1991; Ehleringer and Dawson, 1992; Chen et al., 2020), except in saline or xeric environments (Lin and Sternberg, 1993; Ellsworth and Williams, 2007). Some recent studies showed, however, that the occurrence of isotopic fractionation during root water uptake was probably more common than previously thought, especially with respect to $\delta^{2}H$ values (Zhao et al.,

2016; Wang et al., 2017; Barbeta et al., 2019; Poca et al., 2019; Liu et al., 2021a, 2022).

In addition to plant source water, leaf water is also isotopically enriched through the evaporative process during transpiration. The enrichment of ^{18}O and ^{2}H by leaf water transpiration can be predicted using the Craig-Gordon model (C-G model). This model was initially proposed to describe the evaporative enrichment of a freely evaporating water body (Craig and Gordon, 1965) and has been modified for plant leaves under steady-state conditions (Dongmann et al., 1974; Farquhar and Cernusak, 2005). However, the C-G model fails to explain the intra-leaf heterogeneity of $\delta^{18}O_{leaf}$ and $\delta^{2}H_{leaf}$ (Cernusak et al., 2016; Liu et al., 2021b), which is currently described using a two-pool model (Leaney et al., 1985; Song et al., 2015) and/or an advection-diffusion model, as the *Péclet* effect (Farquhar and Lloyd, 1993; Farquhar and Gan, 2003). Subsequently, more complicated models have been developed to cover non-steady-state conditions (Ogée et al., 2007). These models emphasize a mechanistic understanding of leaf water isotopic fractionation, but the relevant parameters cannot be strictly constrained or precisely monitored, which hinders the use of these models under natural conditions (Plavcová et al., 2018).

This study combined the effects of measured source water isotopes and C-G model-predicted transpiration on $\delta^{18}O_{leaf}$ and $\delta^{2}H_{leaf}$ values. Our objectives were to deepen the understanding of the controls on the $\delta^{18}O_{leaf}$ and $\delta^{2}H_{leaf}$ across different seasons. Based upon these objectives, we repeatedly sampled soils, twigs, and leaves in May, July, and

September (representing spring, summer, and autumn, respectively) from the same ten plots distributed along an elevation transect. Simultaneously, we obtained the relevant meteorological parameters (e.g., temperature, relative humidity, and precipitation) from sites close to the sampling plots along the transect and used these to predict the $\delta^{18}O_{leaf}$ and $\delta^{2}H_{leaf}$ values. The combined analysis of concurrent measurements of $\delta^{18}O$ and $\delta^{2}H$ values in soil water, twig water, and leaf water with the predicted $\delta^{18}O$ and $\delta^{2}H$ values of leaf water from the C-G model associated with the surrounding meteorological parameters will help to identify the factors that control $\delta^{18}O_{leaf}$ and $\delta^{2}H_{leaf}$ values. Furthermore, we performed an isotope-based line analysis of the dual $\delta^{18}O$ and $\delta^{2}H$ values of leaf water, associated with altitude and seasonality. This study will improve our understanding of the environmental signals preserved within the $\delta^{18}O$ and $\delta^{2}H$ values extracted from plant organic biomarkers associated with leaf water.

2. Materials and Methods

2.1 Study area

The Qinling Mountains form the dividing line between northern and southern China and mark the boundary between the watersheds of the Yellow and Yangtze Rivers. Mt. Taibai (Fig. 1; 33. 96 °N, 107.77 °E) rises to 3767 m above sea level (asl) and is the peak in the Qinling Mountains; it has a warm temperate ecosystem characterized by a rich diversity of flora and fauna. The mean annual temperature at the bottom of Mt. Taibai is 12.9°C, and the mean annual precipitation is 609.5 mm (Zhang and Liu, 2010). The climate, soil, and vegetation vary significantly along our slope transect, exhibiting

a remarkable vertical geo-ecological zonation (Fig. 1). The area contains a variety of climate zones: warm temperate (< 1300 m asl), temperate (1300 - 2600 m asl), cool temperate (2600 - 3350 m asl), and alpine (> 3350 m asl). The soil types vary from yellow loess soil at low elevations, spectacular rocky outcrops at middle elevations, and glacial remnants at high elevations. Vegetation along the transect is mainly coniferous and broadleaf forests and alpine and subalpine vegetation (Fig. 1; Liu, 2021). The dominant species range from *Quercus variabilis*, *Q. aliena*, *Betula albosinensis*, *B. utilis*, *Abies fargessi,* and *Larix chinensis* forests to *Rhododendron clementinae* and *R. concinnum* alpine (Supplementary table S1).

2.2 Sampling strategy

Plants and soils were sampled in May, July, and September 2020, and samples were collected from 10 plots (3 × 3 m) covering all of the vegetation zones along the northern slope of Mt. Taibai, extending from 608 to 3533 m asl (Fig. 1). Among the plots, six sites (i.e., sites 2, 3, 4, 5, 8, and 10; Fig. 1) were selected as being the closest to the weather stations along the elevation transect, and they were used in order to obtain the *in-situ* meteorological data for analysis. For the plants, one or two dominant deciduous and coniferous trees were chosen in each plot across the vegetation zone (Supplementary Table S1). Several large leaves and suberized twigs were collected for each species. Three to ten large leaves were chosen for sampling, and a small number were collected in broadleaf forests and a large number in coniferous forests, depending on leaf size. The leaf samples were conducted in the context of the intact leaves because of the likely isotopic gradients within a leaf (Helliker and Ehleringer, 2000; Liu et al.,

2016). Our sampling period was between 12 pm and 3 pm because maximum diurnal enrichment of the leaf water isotopic composition occurs during this part of the day (Romero and Feakins, 2011; Liu et al., 2021). The twigs were collected simultaneously by cutting suberized twigs, and all of the twigs were cut into samples that were 3-4 cm long. The leaf and twig samples were immediately placed into glass vials with screw caps and sealed with polyethylene parafilm. For the soils, three surface soil samples (less than 10 cm deep) were collected from around the sampled plants using a small metal scoop at each plot. All sampling plots were located on slopes far from rivers and surface water bodies, which ensured that the soil water in each plot was derived exclusively from precipitation. Although the surface soil layers were collected only as the representatives of soil water in this study, these samples could provide a relatively good source of water for the plants, as supported by a prior study conducted along the same elevation transect (Zhang and Liu, 2010). The soil samples were tightly sealed in a polyethylene zipper bag on site. All plant and soil samples were stored in a cool box (~ 4 °C) in the field and immediately transported to the laboratory. The altitude of each plot was determined using a handheld GPS unit with an error of ± 5 m.

2.3 Isotope analysis

The water in the plant and soil samples was extracted using an automatic cryogenic vacuum extraction system (LI-2100 Pro, LICA United Technology Limited, Beijing, China). The auto-extraction process was set for 3 hours, and the extraction rate of water from the samples was more than 98%. The isotopic composition of the soil water was measured using a Picarro L2130-I isotope water analyzer (Sunnyvale, CA, USA) at the

State Key Laboratory of Loess and Quaternary Geology, Institute of Earth Environment, Chinese Academy of Sciences. The analytical accuracies were ±0.1‰ for $\delta^{18}O$ and ±1‰ for $\delta^{2}H$. An isotope ratio mass spectrometer was coupled to a high-temperature conversion elemental analyzer (HT2000 EA-IRMS, Delta V Advantage; Thermo Fisher Scientific, Inc. USA) to take isotopic measurements of twig and leaf water at the Huake Precision Stable Isotope Laboratory on the campus of Tsinghua Shenzhen International Graduate School. The measurement precisions were ± 0.2‰ and ± 1‰ for $\delta^{18}O$ and $\delta^{2}H$, respectively. The isotopic composition of $\delta^{18}O$ and $\delta^{2}H$ is expressed as an isotopic ratio:

$$\delta_{sample}(‰) = \left(\frac{R_{sample} - R_{standard}}{R_{standard}}\right) \times 1000 \quad (1)$$

where δ_{sample} represents $\delta^{18}O$ or $\delta^{2}H$, and R_{sample} and $R_{standard}$ indicate the ratio of $^{18}O/^{16}O$ or $^{2}H/^{1}H$ of the sample and standard, respectively. The $\delta^{18}O$ and $\delta^{2}H$ values are reported relative to the Vienna mean standard ocean water (VSMOW). In addition, the mean monthly $\delta^{18}O$ and $\delta^{2}H$ values of precipitation were determined using the Online Isotope in Precipitation Calculator (Bowen and Revenaugh, 2003).

2.4 Modelling isotopes of leaf water

The C-G equation can be approximated as follows (Cernusak et al., 2022):

$$\delta_e = \delta_s + \varepsilon^+ + \varepsilon_k + (\delta_v - \delta_s - \varepsilon_k) \times \frac{e_a}{e_i} \quad (2)$$

where δ_e is the predicted $\delta^{18}O$ and $\delta^{2}H$ values at the evaporative sites within leaves, δ_s is the $\delta^{18}O$ and $\delta^{2}H$ values of source water (equivalent to twig water in our study), ε^+ is the equilibrium fractionation between liquid water and vapour, and ε_k is the kinetic fractionation during the diffusion of vapour through the stomata and the

boundary layer.

In our analysis, we calculated Δ_v (the enrichment of atmospheric vapour relative to source water) as $\Delta_v = (\delta_v - \delta_s)/(1 + \delta_s)$, and the values of Δ_v are often close to $-\varepsilon^+$ at the isotopic steady-state (Barbour, 2007; Cernusak et al., 2016); therefore, we can calculate δ_v as $\delta_v = -\varepsilon^+ + (1 - \varepsilon^+)\delta_s$. In addition, $\frac{e_a}{e_i}$ is the ratio of the water vapour pressure fraction in the air relative to that in the intercellular spaces and is equal to the relative humidity (RH) in the air at steady state (Cernusak et al., 2022). Thus, Equation (2) can be derived as

$$\delta_e = (1 - h)(\varepsilon^+ + \varepsilon_k) + (1 - \varepsilon^+ h)\delta_s \quad (3)$$

where δ_s represents the isotopic values of twig water, and h is the mean annual or monthly RH (MARH or MMRH) in this study. The equilibrium fractionation (ε^+) varies as a function of temperature (Bottinga and Craig, 1969) and can be equated to $\delta^{18}O$ and δ^2H, as follows (Majoube, 1971):

$$\varepsilon_o^+(‰) = \left[\exp\left(\frac{1.137}{(273+T)^2} \times 10^3 - \frac{0.4156}{273+T} - 2.0667 \times 10^{-3}\right) - 1\right] \times 1000 \quad (4)$$

$$\varepsilon_H^+(‰) = \left[\exp\left(\frac{24.844}{(273+T)^2} \times 10^3 - \frac{76.248}{273+T} + 52.612 \times 10^{-3}\right) - 1\right] \times 1000 \quad (5)$$

The kinetic fractionation (ε_k) can be calculated for $\delta^{18}O$ and δ^2H as (Farquhar et al., 2007; Cernusak et al., 2016):

$$\varepsilon_k^O(‰) = \frac{28r_s + 19r_b}{r_s + r_b} \quad (6)$$

$$\varepsilon_k^H(‰) = \frac{25r_s + 17r_b}{r_s + r_b} \quad (7)$$

where r_s and r_b are the resistances of the stomatal and boundary layers, respectively (i.e., the inverse of the conductance of the stomatal and boundary layers). Previous studies found stomatal and boundary layer conductance values of 0.49 and 2.85 mol m^-

^{2} s^{-1}, respectively (Cernusak et al., 2016; Munksgaard et al., 2017), resulting in ε_k^O and ε_k^H values of 26.7 and 23.8, respectively.

2.5 Statistical analysis

Statistical analysis (i.e., the mean, maximum and minimum values, as well as the standard deviation) of the isotopes extracted from the precipitation, soil, twig, and leaf samples was performed to define the range and distribution of the $\delta^{18}O$ and $\delta^{2}H$ values across the seasons. The Pearson correlation method was used to assess the correlations between the $\delta^{18}O$ and $\delta^{2}H$ values among the different water types (i.e., precipitation, soil water, twig water, and leaf water). Hierarchical cluster analysis was used to show the relationships among $\delta^{18}O_{leaf}$ and $\delta^{2}H_{leaf}$ values and potential source water isotopes ($\delta^{18}O$ and $\delta^{2}H$ values in precipitation, soil water, twig water, and leaf water), and meteorological parameters such as mean annual and monthly precipitation (MAP and MMP), mean annual and monthly temperature (MAT and MMT), and mean annual and monthly relative humidity (MARH and MMRH). A one-way analysis of variance (ANOVA) combined with a *post hoc* Tukey's least significant difference (LSD) test was performed to identify the significant differences in the isotopic compositions of precipitation, soil, twig, and leaf waters across the months. Comparisons of the relationships of $\delta^{18}O$ and $\delta^{2}H$ in the soil and leaf water were performed using covariance analysis (ANCOVA) to compare slopes across months. The structural equation model (SEM) was used to explain the respective effects of source waters (i.e., twig water, soil water, and precipitation) and meteorological parameters (i.e., temperature, precipitation, and RH) on $\delta^{18}O_{leaf}$ and $\delta^{2}H_{leaf}$ values. The validated SEMs

generated a good model fit, as indicated by a non-significant χ^2 test ($p > 0.05$), a high comparative fit index (CFI > 0.95), and a low root mean square error of approximation (RMSEA < 0.05). A special SEM was constructed based on the Mantel R values in AMOS (version 24.0.0). Moreover, we used the Hybrid Single-Particle Lagrangian Integrated Trajectory (HYSPLIT) model (Draxler and Rolph, 2003) to calculate air mass back-trajectory for the central site (34.13°N, 107.83°E, 2270 m asl) in the study area. These trajectories were initiated four times daily (at 00:00, 06:00, 12:00, and 18:00 UTC), and their air parcel was released at 2300 m asl for May, July, and September 2020 and moved backwards by winds for 120 h (5 days).

3. Results

3.1 Differing response of $\delta^{18}O$ and $\delta^{2}H$ values of leaf water

The measured $\delta^{18}O$ and $\delta^{2}H$ values of leaf water responded differently to source water isotopes (Fig. 2a) and meteorological parameters (Fig. 2b) across the seasons. The leaf water $\delta^{18}O$ and $\delta^{2}H$ values ($\delta^{18}O_{leaf}$ and $\delta^{2}H_{leaf}$) were clustered with those of the twig water ($\delta^{18}O_{twig}$ and $\delta^{2}H_{twig}$; Fig. 2a) and with MARH, MAT, and MMT (Fig. 2b). The $\delta^{2}H_{leaf}$ values were more closely correlated with isotopes of the potential source waters (e.g., twig water, soil water, and precipitation) than the $\delta^{18}O_{leaf}$ values in different months (Fig. 2a). In contrast, leaf water $\delta^{18}O$ and $\delta^{2}H$ values were correlated with meteorological parameters (Fig. 2b) throughout the study period. These correlations were more significant in summer (July) and autumn (September) than in spring (May).

265 3.2 Comparisons of measured and predicted $\delta^{18}O$ and $\delta^{2}H$ values of leaf water

266 The $\delta^{18}O_{leaf}$ and $\delta^{2}H_{leaf}$ values predicted by the C-G model were compared with the
267 measured $\delta^{18}O$ and $\delta^{2}H$ values across all three months (Fig. 3). The C-G models
268 explained 49% and 70% of the observed variations in the $\delta^{18}O_{leaf}$ and $\delta^{2}H_{leaf}$ values,
269 respectively (Fig. 3a, c). The slopes of the relationships for both $\delta^{18}O$ and $\delta^{2}H$ values
270 of leaf water were less than one, which suggests that part of the bulk leaf water is
271 derived from unenriched vein water. However, there were no significant differences in
272 $\delta^{18}O_{leaf}$ ($p = 0.54$; Fig. 3b) and $\delta^{2}H_{leaf}$ values ($p = 0.93$; Fig. 3d) between the C-G model
273 predicted values and the measured values.

274

275 3.3 Variations of $\delta^{18}O$ and $\delta^{2}H$ values of different waters with seasons and altitude

276 There was a significant correlation between $\delta^{18}O_{leaf}$ and $\delta^{2}H_{leaf}$ values ($R^2 = 0.81$, $p <$
277 0.01; Fig. 4), with significant clusters of $\delta^{18}O_{leaf}$ and $\delta^{2}H_{leaf}$ values across the months,
278 and values were higher in May, intermediate in July, and lower in September (Fig. 4).
279 Within each month, the $\delta^{18}O_{leaf}$ and $\delta^{2}H_{leaf}$ values were depleted in ^{2}H and ^{18}O at higher
280 altitudes relative to lower altitudes. Likewise, the potential types of source water (i.e.,
281 twig water, soil water, and precipitation) exhibited consistent variations across the
282 months, showing values that were relatively higher in May, intermediate in July, and
283 lower in September (Supplementary Fig. S1). The correlations between $\delta^{18}O$ and $\delta^{2}H$
284 values among the source waters were also significant (Supplementary Fig. S2).
285 Nevertheless, the slopes and coefficients of determination (R^2) between the $\delta^{18}O$ and
286 $\delta^{2}H$ values showed a decrease for precipitation, soil water, twig water, and leaf water

from the three sampling months, except for soil water in May (Supplementary Fig. S2). In addition, the ANCOVA showed no significant differences for the regression lines for precipitation (df = 0.47, $F = 2.49$, $p = 0.11 > 0.05$), twig water (df = 53.2, $F = 0.42$, $p = 0.66 > 0.05$), and leaf water (df = 437.3, $F = 2.78$, $p = 0.08 > 0.05$) across study months but a significant difference for soil water across the months (df = 308.8, $F = 10.9$, $p < 0.05$).

4. Discussion

4.1 $\delta^{18}O$ and $\delta^{2}H$ values of leaf water

A recent global meta-analysis indicated that $\delta^{18}O_{leaf}$ and $\delta^{2}H_{leaf}$ values reflect environmental drivers differently and showed that $\delta^{2}H_{leaf}$ values more strongly reflect xylem water and atmospheric vapour $\delta^{2}H$ values, whereas $\delta^{18}O_{leaf}$ values more strongly reflect air relative humidity (Cernusak et al., 2022). Seasonal and localized observations along an elevation transect on the Chinese Loess Plateau supported these different responses of $\delta^{18}O_{leaf}$ and $\delta^{2}H_{leaf}$ to the isotopic composition of the source water and meteorological conditions (Fig. 2). This is likely due to the variation in precipitation isotopic values compared with that in leaf water evaporative enrichment is larger for $\delta^{2}H_{leaf}$ than $\delta^{18}O_{leaf}$ (Cernusak et al., 2022). In addition, we found stronger correlations between $\delta^{2}H_{leaf}$ and isotope values of the source water (twig water, soil water, and precipitation) than between $\delta^{18}O_{leaf}$ values and the source water isotope values (Fig. 2a). This is consistent with the global meta-analysis results (Cernusak et al., 2022). However, our localized study did not show a significantly different response of $\delta^{18}O_{leaf}$ and $\delta^{2}H_{leaf}$

values to meteorological parameters, which responded at almost equivalent magnitudes (Fig. 2b). These observations suggest that plant organic isotopic proxies such as leaf wax (Sachse et al., 2012; Liu et al., 2016) and cellulose (Barbour, 2007; Lehman et al., 2017), which originate from $\delta^{18}O_{leaf}$ and $\delta^{2}H_{leaf}$ values, can provide comparative information that indicates climatic signals (e.g., temperature, RH, and precipitation) in natural archives. These results argued with the recent global meta-analysis that $\delta^{18}O_{leaf}$ and $\delta^{2}H_{leaf}$ values reflect climatic parameters (i.e., RH and temperature) differently (Cernusak et al., 2022). The stronger correlations for $\delta^{2}H_{leaf}$ values than $\delta^{18}O_{leaf}$ values with isotopic values of the source water were likely because the $\delta^{2}H_{leaf}$ values are ultimately determined only by precipitation $\delta^{2}H$ (Sachse et al., 2012; Liu et al., 2016), whereas the $\delta^{18}O_{leaf}$ values are affected by a mixture of precipitation $\delta^{18}O$ and atmospheric factors (O_2 and CO_2) (Barbour, 2007; Cernusak et al., 2016). However, the comparative responses of both $\delta^{2}H_{leaf}$ and $\delta^{18}O_{leaf}$ values to climatic parameters were probably due to the same conditions surrounding the leaf.

The results of the cluster analysis showed that the isotope values of leaf water ($\delta^{18}O_{leaf}$ and $\delta^{2}H_{leaf}$) and twig water ($\delta^{18}O_{twig}$ and $\delta^{2}H_{twig}$) were clustered into one group, but those of soil water ($\delta^{18}O_{soil}$ and $\delta^{2}H_{soil}$) and precipitation ($\delta^{18}O_{p}$ and $\delta^{2}H_{p}$) were clustered into another (Fig. 2a). This indicates that the direct source water of $\delta^{18}O_{leaf}$ and $\delta^{2}H_{leaf}$ should be $\delta^{18}O_{twig}$ and $\delta^{2}H_{twig}$, providing the source water isotope basis for the C-G model. In the C-G model (see Equation 2), besides the source water isotopes, the equilibrium fractionation factor (ε^{+}) and atmospheric vapour enrichment (Δ_v)

depend on the temperature at the isotopic steady-state. Thus, the $\delta^{18}O_{leaf}$ and $\delta^{2}H_{leaf}$ values were predicted to be associated primarily with temperature, RH, and source water, which is consistent with the results from the cluster analysis that the $\delta^{18}O_{leaf}$ and $\delta^{2}H_{leaf}$ values were clustered with temperature (MAT and MMT) and RH (MARH; Fig. 2b). Based on the C-G model, we plotted the measured and predicted $\delta^{18}O_{leaf}$ and $\delta^{2}H_{leaf}$ values (Fig. 3a, c) and observed no significant differences between them (Fig. 3b, d). This is because our three-repeated samplings occur during the day when leaf water is generally near an isotopic steady-state when chloroplasts are mostly located near the evaporative sites (Cernusak et al., 2016). The non-steady state effects on leaf water isotopes were expected at night because of low stomatal conductance (Cernusak et al., 2005; Cuntz et al., 2002; Cernusak et al., 2016). Although the slopes of the predicted and measured $\delta^{18}O_{leaf}$ and $\delta^{2}H_{leaf}$ values were less than one, the C-G model still provides a reasonable framework for guiding the analysis of the different controls on $\delta^{18}O_{leaf}$ and $\delta^{2}H_{leaf}$ values.

4.2 Dual $\delta^{18}O$ and $\delta^{2}H$ plots of leaf water

There was a significant linear correlation between the $\delta^{18}O_{leaf}$ and $\delta^{2}H_{leaf}$ values, with remarkable clusters associated with the three months studied (Fig. 4). As is well-known, the LMWL, generated by precipitation $\delta^{18}O$ and $\delta^{2}H$ values at the local scale, serves as an important reference line for intercomparisons of different waters. Furthermore, the regression lines of the $\delta^{18}O$ and $\delta^{2}H$ values from soil water, twig water, and leaf water (Supplementary Fig. S2) suggest that the leaf water isotopes could well inherit isotopic

353 signals of source waters that originate from twig water, soil water, and ultimately
354 precipitation. The slopes and intercepts of the $\delta^{18}O$ and $\delta^{2}H$ values decreased
355 significantly from precipitation, soil water, twig water, and leaf water for each month,
356 except for soil water in May (Supplementary Fig. S2). Such patterns have been
357 observed in many previous calibration studies (Brooks et al., 2010; Evaristo et al., 2015;
358 Sprenger et al., 2016, 2017; Wang et al., 2017; Benettin et al., 2018; Barbeta et al., 2019;
359 Penna and Meerveld, 2019; Liu et al., 2021a, 2022). The slopes of the LMWLs were
360 lower in July (6.79) than in May (7.04) and September (6.85), but were not significantly
361 different (ANCOVA test: df = 0.47, $F = 2.49$, $p = 0.11 > 0.05$). This suggests that the
362 local water vapour from precipitation was derived from the same source across the
363 seasons, but was subject to different intensities of evaporation as the temperature
364 changed throughout the seasons (Li et al., 2019; Wu et al., 2019, 2021). The slopes of
365 the $\delta^{18}O$ and $\delta^{2}H$ values from the soil, twig, and leaf waters were much smaller than the
366 LMWLs across the study months due to the secondary evaporation in the other water
367 types.
368
369 In the dual isotope plot of leaf water, there were well-defined clusters of $\delta^{18}O_{leaf}$ and
370 $\delta^{2}H_{leaf}$ values across the three months: ^{18}O and ^{2}H were depleted in September, there
371 were intermediate values in July, and ^{18}O and ^{2}H were enriched in May (Fig. 4). When
372 focusing on each month, relatively higher isotopic values occurred at low elevations,
373 but lower isotopic values were present at high elevations despite there being no, or only
374 weak, correlations between the $\delta^{18}O_{leaf}$ and $\delta^{2}H_{leaf}$ values and altitude (Supplementary

375 Fig. S3). The correlations between the $\delta^{18}O_{leaf}$ and $\delta^{2}H_{leaf}$ values and altitude, and
376 between the $\delta^{18}O_{twig}$ and $\delta^{2}H_{twig}$ values and altitude, were not significant across the three
377 months; however, the $\delta^{18}O_{p}$ and $\delta^{2}H_{p}$, and also the $\delta^{18}O_{soil}$ and $\delta^{2}H_{soil}$ values, were
378 significantly correlated with altitude (Supplementary Fig. S3), indicating that besides
379 source water (precipitation and soil water), other factors associated with plants also
380 affect $\delta^{18}O_{leaf}$ and $\delta^{2}H_{leaf}$ values.
381
382 The dual isotope plot of $\delta^{18}O_{leaf}$ and $\delta^{2}H_{leaf}$ values shows a significant isotope line, y =
383 $4.52x$ - 50.7 (R^2 = 0.81, p < 0.01; Fig. 4), but shallower slopes (3.53, 1.86, and 2.81 in
384 May, July, and September, respectively) of $\delta^{18}O_{leaf}$ and $\delta^{2}H_{leaf}$ values were observed
385 across the seasons (Supplementary Fig. S2). Such a correlation was supported by a
386 recent study that conducted consecutive measurements of $\delta^{18}O$ and $\delta^{2}H$ values in
387 xylem/leaf water in Switzerland and indicated that leaf water provided great potential
388 to determine the source water of plants (Benettin et al., 2021). Our study showed
389 remarkable clusters in the measured (Fig. 4) and the C-G model predicted (Fig. 3)
390 $\delta^{18}O_{leaf}$ and $\delta^{2}H_{leaf}$ values across the months and the consistencies of respective $\delta^{18}O_{leaf}$
391 and $\delta^{2}H_{leaf}$ values with potential source water isotopes across months (Supplementary
392 Fig. S1). These findings of temporally consistent dynamics among the water types (i.e.,
393 precipitation, soil water, twig/stem water, and leaf water) have been observed in a
394 number of previous studies (Phillips and Ehleringer, 1995; Cernusak et al., 2005;
395 Sprenger et al., 2016; Berry et al., 2017; Liu et al., 2021a).
396

The isotopic inheritance from precipitation to leaf water indicates that seasonal variations of $\delta^{18}O_p$ and $\delta^{2}H_p$ values are the first-order control on the temporal patterns observed in leaf water. The seasonal dynamics of the $\delta^{18}O_p$ and $\delta^{2}H_p$ values reflect the combined effects of factors such as temperature, altitude, and precipitation amount, which are associated with orographic conditions, as well as sub-cloud evaporation, moisture recycling, and differences in the vapor source (Dansgaard, 1964; McGuire and McDonnell, 2007; Li et al., 2016; Penna and Meerveld, 2019; Wu et al., 2019). In this study, we used the HYSPLIT model to demonstrate the ultimate cause of the seasonal variations of $\delta^{18}O_{leaf}$ and $\delta^{2}H_{leaf}$ values; that is, the monthly dynamics of the $\delta^{18}O_p$ and $\delta^{2}H_p$ values. The monthly variations of the $\delta^{18}O_p$ and $\delta^{2}H_p$ values from the Global Network for Isotopes in Precipitation (GNIP, http://www.iaea.org/) at Xi'an station (1985-1992 AD), which is ~100 km from our study transect, were enriched in ^{18}O and ^{2}H in May relative to July and September (Fig. 5a, b). The cluster mean of the moisture transport routes from HYSPLIT (Draxler and Rolph, 2003) and the climatological 850 hPa wind vectors showed that the primary moisture sources were from western China and central Asia in May, the China-India Peninsula and Bay of Bengal, and local moisture recycling and convection (Fig. 5c, d, e). The seasonal variations in $\delta^{18}O_p$ and $\delta^{2}H_p$ values are consistently related to the onset, advancement, and retreat of the Asian summer monsoon and associated changes in the large-scale monsoon circulation (e.g., Zhang et al., 2020, 2021). As the summer monsoon starts in mid-May, the rainfall season starts in southern China; however, our study area is controlled mainly by moisture from the westerlies (Chiang et al., 2015) with relatively higher vapour, $\delta^{18}O_p$,

and δ^2H_p values (Fig. 5c, a, b). In July, the summer monsoon reaches its strongest phase, and the rainfall belt shifts to central and northern China, where the southerly wind brings plenty of moisture from the China-India Peninsula and the Bay of Bengal with lower vapour, $\delta^{18}O_p$, and δ^2H_p values (Fig. 5d, a, b). When the summer monsoon withdraws in September, the study area is controlled mainly by local moisture recycling and convection (Fig. 5e). Soil water, stored after the June-August monsoon rainfall with its lower $\delta^{18}O$ and δ^2H values, results in even lower $\delta^{18}O_p$ and δ^2H_p values in September than in July (Supplementary Fig. S1), casusing significantly lower $\delta^{18}O$ and δ^2H values of leaf water (Fig. 4).

4.3 Framework of controls for $\delta^{18}O$ and δ^2H values of leaf water

To delineate the mechanisms that control the $\delta^{18}O_{leaf}$ and δ^2H_{leaf} values, we used the SEMs to quantify the complex interactions among $\delta^{18}O_{leaf}$ or δ^2H_{leaf} values, source waters, and meteorological parameters (Fig. 6). The coefficients of determination (R^2) were 0.48 and 0.71 for the $\delta^{18}O_{leaf}$ and δ^2H_{leaf} values, respectively, indicating that the models explained more variance for δ^2H_{leaf} values than $\delta^{18}O_{leaf}$ values (Fig. 6). The SEMs showed that potential source waters (i.e., twig water, soil water, and precipitation) had stronger effects on δ^2H_{leaf} relative to $\delta^{18}O_{leaf}$ values, while the meteorological parameters showed weak effects on both $\delta^{18}O_{leaf}$ and δ^2H_{leaf} values (a little larger for δ^2H_{leaf} than $\delta^{18}O_{leaf}$ values). This is consistent with our above correlation analysis (Fig. 2). Surprisingly, the MMT had significant effects on $\delta^{18}O_p$ and δ^2H_p values, suggesting that temperature plays a key role in determining $\delta^{18}O_p$ and δ^2H_p values, but this finding

441 is not discussed further here. Collectively, the SEMs also showed that source water
442 exerts the first-order control but affects $\delta^{18}O_{leaf}$ and $\delta^{2}H_{leaf}$ differently; the
443 meteorological parameters had a weak control on $\delta^{18}O_{leaf}$ and $\delta^{2}H_{leaf}$, with a more
444 substantial effect on $\delta^{2}H_{leaf}$ than $\delta^{18}O_{leaf}$ values.
445
446 A schematic representation of the controls on $\delta^{18}O_{leaf}$ and $\delta^{2}H_{leaf}$ values (respective and
447 dual) is shown in Fig. 7. It involves multiple processes associated with the
448 hydroclimatic and biochemical factors that affect $\delta^{18}O_{leaf}$ and $\delta^{2}H_{leaf}$ values. The
449 meteorological parameters (temperature, RH, and precipitation) exerted distinct effects
450 on the $\delta^{18}O$ and $\delta^{2}H$ values of the source water and, thus, on the $\delta^{18}O_{leaf}$ and $\delta^{2}H_{leaf}$
451 values, as demonstrated above by the SEM. Significant isotopic fractionation occurred
452 mainly at two key locations across the vertical soil profiles and leaf architectures from
453 precipitation to leaf water. First, an isotopic gradient across the vertical soil profile
454 appeared because of evaporation from the surface soil layers (Ehleringer et al., 1992;
455 Goldsmith et al., 2012; Evaristo et al., 2015). This evaporative isotopic fractionation
456 causes a linearly isotopic trajectory down the soil profile (Goldsmith et al., 2012;
457 Rothfuss and Javaux, 2017; Wu et al., 2018; Wang et al., 2019; Amin et al., 2020; Zhao
458 et al., 2020; Liu et al., 2021a). Second, there were significant isotopic heterogeneities
459 because of transpiration associated with the $\delta^{18}O_{leaf}$ (Helliker and Ehleringer, 2000;
460 Farquhar and Gan, 2003; Gan et al., 2003; Song et al., 2015) and $\delta^{2}H_{leaf}$ values
461 (Šantrůček et al., 2007; Liu et al., 2016; Liu et al., 2021b) within a leaf, which depends
462 substantially on veinal structures (Liu et al., 2021b). The within-leaf heterogeneity of

463 the $\delta^{18}O_{leaf}$ and $\delta^{2}H_{leaf}$ values can be explained using the *Péclet*-modified C-G model
464 (Gan et al., 2003; Farquhar and Gan, 2003; Cernusak et al., 2005, 2016). Collectively,
465 the soil evaporation and leaf transpiration produce isotopic enrichment above source
466 water (precipitation or soil water). Soil evaporation leads to an isotopic gradient across
467 the vertical soil profile, providing water sources for plant root uptake without isotope
468 fractionation during the process (Dawson and Ehleringer, 1991; Ehleringer and Dawson,
469 1992; Chen et al., 2020). During water transport between roots and leaf petioles,
470 isotopic compositions of xylem water remain unaltered from those in soils (i.e., soil
471 immobile water), until it reaches the leaf, which undergoes water loss (Ehleringer and
472 Dawson, 1992). Within the leaf, transpiration leads to significant isotopic enrichment
473 (Helliker and Ehleinger, 2000; Liu et al., 2015; Cernusak et al., 2016), which is highly
474 dependent on meteorological parameters (e.g., temperature and relative humidity).
475 However, the meteorological parameters varied with altitude and seasonality, yielding
476 an isotopic water line (LWL) in the dual-isotope plot (Fig. 4). The LWL provides an
477 important baseline for leaf-derived organic matter such as cellulose (e.g., Barbour, 2007;
478 Lehman et al., 2017) and leaf wax (Liu et al., 2016, 2021). Overall, the LWL is
479 controlled primarily by altitude and seasonality, as these are the main influencers of the
480 hydroclimatic factors.
481

482 ## 5 Conclusion

483 Along an elevation transect on the Chinese Loess Plateau, precipitation, soil water, twig
484 water, and leaf water were repeatedly sampled to explore the controls on $\delta^{18}O_{leaf}$ and

485 δ^2H_{leaf} values associated with meteorological parameters and source water. The effects
486 of meteorological parameters and source water on $\delta^{18}O_{leaf}$ and δ^2H_{leaf} values were
487 different, and the dual $\delta^{18}O_{leaf}$ and δ^2H_{leaf} plot generated an isotopic line. We found that
488 δ^2H_{leaf} values were more closely correlated with source water isotopes than $\delta^{18}O_{leaf}$
489 values, whereas $\delta^{18}O_{leaf}$ and δ^2H_{leaf} values were similarly correlated with
490 meteorological parameters along the elevation transect. The observations suggest that
491 plant organic isotopic proxies such as leaf wax and cellulose originating from $\delta^{18}O_{leaf}$
492 and δ^2H_{leaf} values can provide comparative climatic information on the Loess Plateau
493 of China. Additionally, the dual-isotope analysis showed that the $\delta^{18}O_{leaf}$ and δ^2H_{leaf}
494 values were closely correlated because of their similar altitudinal and seasonal
495 responses. The first-order control on $\delta^{18}O_{leaf}$ and δ^2H_{leaf} values was the source water
496 (i.e., precipitation), and the meteorological parameters had a comparable effect on both
497 $\delta^{18}O_{leaf}$ and δ^2H_{leaf} values, which varied with altitude and season across the transect on
498 the Loess Plateau. In the future, we will investigate the relationships of intersection
499 angle θ with hydroclimatic and biochemical factors.
500

501 **Competing interests**

502 The authors declare that they have no known competing financial interests or personal
503 relationships that could have appeared to influence the work reported in this paper.
504

505 **Acknowledgment**

506 We thank X. Cao and M. Xing for help with laboratory assistance, and Y. Cheng for the

help in the field. We thank Profs. J. J. McDonnell and L. A. Cernusak for discussing and editing the paper. We also thank Shaanxi Meteorological Bureau for supporting meteorological data along an elevation transect. This work was supported by the National Natural Science Foundation of China (42073017) and the Chinese Academy of Sciences (XAB2019B02; XDB40000000; ZDBS-LY-DQC033; 132B61KYSB20170005) .

Author contribution

J.L. conceived the idea of research, and performed the data analysis. J.L., H.W., and H.Z. wrote the manuscript. L.G. and Y.Z. edited the paper. J.L. and C.J. performed the lab work. All authors contributed to discuss the results.

Data availability statement

Data related to this article can be found in Electric Annex and Mendeley Data (https://data.mendeley.com/drafts/t44wybgpr3).

References

Amin, A., Zuecco, G., Geris, J., Schwendenmann, L., McDonnell, J.J., Borga, M., and Penna, D.: Depth distribution of soil water sourced by plants at the global scale: a new direct inference approach, Ecohydrology, 13, e2177, 2020.

Allison, G., Barnes, C., and Hughes, M.: The distribution of deuterium and ^{18}O in dry soils 2. Experimental, J. Hydrol., 64, 377–397, 1983.

529 Barbeta, A., Jones, S. P., Clavé, L., Gimeno, T. E., Fréjaville, B., Wohl, S., and Ogée,
530 J.: Unexplained hydrogen isotope offsets complicate the identification and
531 quantification of tree water sources in a riparian forest, Hydrol. Earth Syst. Sci., 23,
532 2129–2146, 2019.
533 Barbour, M. M.: Stable oxygen isotope composition of plant tissue: a review. Funct.
534 Plant Biol., 34, 83–94, 2007.
535 Barbour, M. M., Farquhar, G. D., and Buckley, T. N.: Leaf water stable isotopes and
536 water transport outside the xylem, Plant Cell Environ., 40, 914–920, 2017.
537 Benettin, P., Nehemy, M. F., Cernusak, L. A., Kahmen, A., and McDonnell, J. J.: On
538 the use of leaf water to determine plant water source: A proof of concept, Hydrol.
539 Process., DOI: 10.1002/hyp.14073, 2021.
540 Benettin, P., Volkmann, T. H. M., von Freyberg, J., Frentress, J., Penna, D., Dawson, T.
541 E., and Kirchner, J. W.: Effects of climatic seasonality on the isotopic composition of
542 evaporating soil waters, Hydrol. Earth Syst. Sci., 22, 2881–2890, 2018.
543 Berry, Z. C., Evaristo, J., Moore, G., Poca, M., Steppe, K., Verrot, L., Asbjornsen, H.,
544 Borma, L. S., Bretfeld, M., Herve-Fernandez, P., Seyfried, M., Schwendenmann, L.,
545 Sinacore, K., Wispelaere, L. D., and McDonnell, J.: The two water worlds hypothesis:
546 addressing multiple working hypotheses and proposing a way forward, Ecohydrology,
547 e1843, 2017.
548 Bottinga, Y., and Craig., H.: Oxygen isotope fractionation between CO_2 and water, and
549 the isotopic composition of marine atmospheric CO_2, Earth Planet. Sci. Lett., 5, 285–
550 295, 1969.

551 Bowen, G. J., and Revenaugh, J.: Interpolating the isotopic composition of modern
552 meteoric precipitation, Water Resour. Res., 39, 1299, 2003.
553 Bowen, G. J.: Isoscapes: Spatial pattern in isotopic biogeochemistry, Annu. Rev. Earth
554 Planet. Sci., 2010, 161–187, 2010.
555 Bowen, G. J., and Good, S. P.: Incorporating water isoscapes in hydrological and water
556 resource investigations, Wiley Interdiscip. Rev. Water, 2, 107–119, 2015.
557 Brooks, J. R., Barnard, H. R., Coulombe, R., and McDonnell, J. J.: Ecohydrologic
558 separation of water between trees and streams in a Mediterranean climate, Nat. Geosci.,
559 3, 100–104. 2010.
560 Cernusak, L. A., Farquhar, G. D., and Pate, J. S.: Environmental and physiological
561 controls over oxygen and carbon isotope composition of Tasmanian blue gum,
562 *Eucalyptus globulus*, Tree Physiol., 25, 129–146, 2005.
563 Cernusak, L. A., Barbour, M. M., Arndt, S. K., Cheesman, A. W., English, N. B., field,
564 T. S., Helliker, B. R., Holloway-Phillips, M. M., Holtum, J. A. M., Kahmen, A.,
565 McInerney, F. A., Munksgaard, N. C., Simonin, K. A., Song, X., Stuart-Williams, H.,
566 West, J. B., and Farquhar, G. D.: Stable isotopes in leaf water of terrestrial plants. Plant
567 Cell Environ., 39, 1087–1102, 2016.
568 Cernusak, L. A., Barbeta, A., Bush, R., Eichstaedt R., Ferrio, J., Flanagan, L., Gessler,
569 A., Martín-Gómez, P., Hirl, R., Kahmen, A., Keitel., C., Lai, C., Munksgaard, N.,
570 Nelson, D., Ogée J., Roden, J., Schnyder, H., Voelker, S., Wang L., Stuart-Williams, H.,
571 Wingate, L., Yu, W., Zhao, L., Cuntz, M., 2022. Do ^{2}H and ^{18}O in leaf water reflect
572 environmental drivers differently? New Phytologist, DOI: 10.1111/nph.18113.

573 Chen. Y., Helliker, B. R., Tang, X., Li, F., Zhou, Y., and Song, X.: Stem water cryogenic
574 extraction biases estimation in deuterium isotope composition of plant source water,
575 Proc. Natl. Acad. Sci., 117, 33345–33350, 2020.
576 Chiang, J. C., Fung, I. Y., Wu, C. -H., Cai, Y., Edman, J. P., Liu, Y., Day, J. A.,
577 Bhattacharya, T., Mondal, Y., and Labrousse, C. A.: Role of seasonal transitions and
578 westerly jets in East Asian paleoclimate, Quat. Sci. Rev., 108, 111–129, 2015.
579 Craig, H., and Gordon, L. I.: Deuterium and oxygen-18 variations in the ocean and the
580 marine atmosphere. In 'Proceedings of a conference on stable isotopes in
581 oceanographic studies and paleotemperatures', pp. 9–130, 1965.
582 Cuntz M., Ogée J., Farquhar G.D., Peylin P. & Cernusak L.A.: Modelling advection
583 and diffusion of water isotopologues in leaves. Plant Cell Environ. 30, 892–909, 2007.
584 Dansgaard, W.: Stable isotopes in precipitation, Tellus, 16, 436–468, 1964.
585 Dawson, T. E. and Ehleringer, J. R.: Streamside trees that do not use stream water,
586 Nature, 350, 335–337, 1991.
587 Dongmann. G., Nurnberg, H. E., Forstel, H., and Wagener, K.: On the enrichment of
588 $H_2{}^{18}O$ in the leaves of transpiring plants, Radiat. Environ. Biophys. 11, 41–52, 1974.
589 Draxler, R. R., and Rolph, G. D.: HYSPLIT (Hybrid Single-Particle Lagrangian
590 Integrated Trajectory) Model Access via NOAA ARLREADY. htmlNOAA Air
591 Resources Laboratory, http://www.arl.noaa.gov/ready/hysplit4, 2003.
592 Ehleringer, J. R. and Dawson, T. E: Water uptake by plants: perspectives from stable
593 isotope composition, Plant Cell Environ., 15, 1073–1082, 1992.
594 Ehleringer, J. R. and Dawson, T. E.: Water uptake by plants: perspectives from stable

595 isotope composition, Plant Cell Environ., 15, 1073–1082, 1992.
596 Ellsworth, P. Z., and Williams, D. G.: Hydrogen isotope fractionation during water
597 uptake by woody xerophytes, Plant Soil, 291, 93–107, 2007.
598 Evaristo J., Jasechko S., and McDonnell J. J.: Global separation of plant transpiration
599 from groundwater and streamflow, Nature, 525, 91–94, 2015.
600 Farquhar, G. D., Cernusak, L. A., and Barnes, B.: Heavy water fractionation during
601 transpiration, Plant Physiol., 143, 11–18, 2007.
602 Farquhar, G. D., and Cernusak, L. A.: On the isotopic composition of leaf water in the
603 non- steady state, Funct. Plant Biol., 32, 293–303, 2005.
604 Farquhar, G..D., and Gan, K..S.: On the progressive enrichment of the oxygen isotopic
605 composition of water along leaves, Plant Cell Environ., 26, 801–819, 2003.
606 Farquhar, G. D., and Lloyd, J.: Carbon and oxygen isotope effects in the exchange of
607 carbon dioxide between terrestrial plants and the atmosphere. In Stable Isotopes and
608 Plant Carbon–Water Relations (eds J.R. Ehleringer, A.E. Hall, & G.D. Farquhar), pp.
609 47–70. Academic Press, San Diego, 1993.
610 Gan, K.S., Wong, S.C., Yong, J.W.H., Farquhar, G.D., 2003. Evaluation of models of
611 leaf water^{18}O enrichments of spatial patterns of vein xylem, leaf water and dry matter
612 in maize leaves. Plant Cell Environ. 26, 1479–1495.
613 Goldsmith, G. R., Munoz-Villers, L. E., Holwerda, F., McDonnell, J. J., Asbjornsen, H.,
614 and Dawson, T. E.: Stable isotopes reveal linkages among ecohydrological processes in
615 a seasonally dry tropical montane cloud forest, Ecohydrology, 5, 779–790, 2012.
616 Helliker, B. R., and Ehleringer, J. R.: Establishing a grassland signature in veins: ^{18}O in

617 the leaf water of C_3 and C_4 grasses, Proc. Natl. Acad. Sci., 97, 7894–7898, 2000.
618 Hepp, J., Schäfer, I. K., Lanny, V., Franke, J., Blidtner, M., Rozanski, K., Glaser, B.,
619 Zech, M., Eglinton, T. I., and Zech, R.: Evaluation of bacterial glycerol dialkyl glycerol
620 tetraether and ^{2}H-^{18}O biomarker proxies along a central European topsoil transect,
621 Biogeosciences, 17, 741–756, 2020.
622 Kahmen, A., Sachse, D., Arndt, S. K., Tu, K. P., Farrington, H., Vitousek, P. M., and
623 Dawson, T. E.: Cellulose $\delta^{18}O$ is an index of leaf-to-air vapor pressure difference (VPD)
624 in tropical plants, Proc. Natl. Acad. Sci., 108, 1981–1986, 2011.
625 Leaney, F., Osmond, C., Allison, G., and Ziegler, H.: Hydrogen-isotope composition of
626 leaf water in C_3 and C_4 plants: its relationship to the hydrogen-isotope composition of
627 dry matter, Planta, 164, 215–220, 1985.
628 Lehmann, M. M., Gamarra, B., Kahmen, A., Siegwolf, R. T. W., and Saurer, M.:
629 Oxygen isotope fractionations across individual leaf carbohydrates in grass and tree
630 species. Plant Cell Environ., 40, 1658–1670, 2017.
631 Li, Z., Feng, Q., Wang, Q., Kong, Y., Cheng, A., Yong, S., Li, Y., Li, J., and Guo, X.:
632 Contributions of local terrestrial evaporation and transpiration to precipitation using
633 $\delta^{18}O$ and D-excess as a proxy in Shiyang inland river basin in China, Global Planet.
634 Change, 146, 140–151, 2016.
635 Li, Z., Li, Z., Yu, H., Song, L., and Ma, J.: Environmental significance and zonal
636 characteristics of stable isotope of atmospheric precipitation in arid Central Asia. Atmos.
637 Res., 227, 24–40, 2019.
638 Lin, G. H., and Sternberg, L. S. L.: Hydrogen isotopic fractionation by plant roots

during water uptake in coastal wetland plants. Stable Isotopic and Plant Carbon/Water Relations, Academic Press, New York, pp. 497–510, 1993.

Liu, J., Liu, W., and An, Z.: Insight into the reasons of leaf wax $\delta D_{n\text{-alkane}}$ values between grasses and woods, Sci. Bull., 60, 549–555, 2015.

Liu, J., Liu, W., An, Z., and Yang, H.: Different hydrogen isotope fractionations during lipid formation in higher plants: Implications for paleohydrology, Sci. Report, 6, 19711, 2016.

Liu, J., Wu, H., Cheng, Y., Jin, Z., and Hu, J.: Stable isotope analysis of soil and plant water in a pair of natural grassland and understory of planted forestland on the Chinese Loess Plateau, Agr. Water Manage., 249, 106800, 2021a.

Liu, J., An, Z., and Lin, G.: Intra-leaf heterogeneities of hydrogen isotope compositions in leaf water and leaf wax of monocots and dicots, Sci. Total Environ., 770, 145258, 2021b.

Liu, J.: Seasonality of the altitude effect on leaf wax n-alkane distributions, hydrogen and carbon isotopes along an arid transect in the Qinling Mountains. Sci. Total Environ., 778, 146272, 2021.

Liu, J., Jiang, C., Guo, L., Hu, J: Ecohydrological separation in a pair catchments covered with natural grassland and planted forestland on the Chinese Loess Plateau: Evidence from a one-year stable isotope observation. Hydrol. Process. 36, e14778, 2022.

Majoube, M: Fractionnement en oxygen-18 et en deuterium entre l'eau et sa vapeur. Journal de Chimie et Physique 68, 1423–1436, 1971.

McGuire, K., and McDonnell J. J.: Stable isotope tracers in watershed hydrology, in Stable Isotopes in Ecology and Environmental Science, Ecological Methods and Concepts Series, pp. 334–374, 2007.

Munksgaard, N. C., Cheesman, A. W., English, N. B., Zwart, C., Kahmen, A., and Cernusak, L. A.: Identifying drivers of leaf water and cellulose stable isotope enrichment in Eucalyptus in northern Australia, Oecologia, 183, 31–43, 2017.

Ogée, J., Cuntz, M., Peylin, P., Bariac, T., 2007. Non-steady-state, non-uniform transpiration rate and leaf anatomy effects on the progressive stable isotope enrichment of leaf water along monocot leaves. Plant Cell Environ. 30, 367–387.

Pagani, M., Pedentchouk, N., Huber, M., Sluijs, A., Schouten, S., Brinkhuis, H., Damsté, J. S. S., and Dichens, G. R.: Arctic hydrology during global warming at the Palaeocene/Eocene thermal maximum, Nature, 442, 671–675, 2006.

Penna, D., and van Meerveld, H. J.: Spatial variability in the isotopic composition of water in small catchments and its effect on hydrograph separation, WIREs Water, e1367, 2019.

Phillips, S. L., and Ehleringer, J. R.: Limited uptake of summer precipitation by big tooth maple (*Acer grandidentatum* Nutt) and Gambels oak (*Quercus gambelii* Nutt), Trees, 9, 214–219, 1995.

Plavcová, L., Hronková, M., Šimková, M., Květoň, J., Vráblová, M., Kubásek, J., Šantrůček, J.: Seasonal variation of $\delta^{18}O$ and $\delta^{2}H$ in leaf water of *Fagus sylvatica* L. and related water compartments, J. Plant Physiol., 227, 56–65, 2018.

Poca, M., Coomans, O., Urcelay, C., Zeballos, S. R., Bodé, S., and Boecks, P.: Isotope

683 fractionation during root water uptake by *Acacia caven* is enhanced by arbuscular
684 mycorrhizas, Plant Soil, 441, 485–497, 2019.
685 Romero, I.C., Feakins, S.I., 2011. Spatial gradients in plant leaf wax D/H across a
686 coastal salt marsh in southern California. Org. Geochem. 42, 618–629.
687 Rothfuss, Y., and Javaux, M.: Reviews and syntheses: isotopic approaches to quantify
688 root water uptake: a review and comparison of methods, Biogeosciences, 14, 2199–
689 2224, 2017.
690 Sachse, D., Billault, I., Bowen, G.J., Chikaraishi, Y., Dawson, T.E., Feakins, S.J.,
691 Freeman, K.H., Magill, C.R., McInerney, F.A., van der Meer, M.T.J., Polissar, P.J.,
692 Robins, R.J., Sachs, J.P., Schmidt, H.L., Sessions, A.L., White, J.W.C., West, J.B.,
693 Kahmen, A., 2012. Molecular paleoyhydrology: interpreting the hydrogen-isotopic
694 composition of lipid biomarkers from photosynthesizing organisms. Annu. Rev. Earth
695 Planet. Sci. 40, 221–249.
696 Šantrůček, J., Květoň, J., Šetlík, J., Bulíčková, L., 2007. Spatial variation of deuterium
697 enrichment in bulk water of snowgun leaves. Plant Physiol. 143, 88–97.
698 Song, X., Loucos, K. E., Simonin, K. A., Farquhar, G. D., and Barbour, M. M.:
699 Measurements of transpiration isotopologues and leaf water to assess enrichment
700 models in cotton, New Phytol., 206, 637–646, 2015.
701 Schefuβ, E., Kuhlmann, H., Mollenhauer, G., Prange, M., and Pätzold, J.: Forcing of
702 wet phases in Southeast Africa over the past 17,000 year, Nature, 480, 22–29, 2011.
703 Sprenger, M., Leistert, H., Gimbel, K., and Weiler, M.: Illuminating hydrological
704 processes at the soil-vegetation-atmosphere interface with water stable isotopes, Rev.

Geophys., 54, 674–704, 2016.

Sprenger, M., Tetzlaff, D., and Soulsby, S.: Soil water stable isotopes reveal evaporation dynamics at the soil-plant-atmosphere interface of the critical zone, Hydrol. Earth Syst. Sci., 21, 3839–3858, 2017.

Wang, J., Fu, B., Lu, N., and Zhang, L.: Seasonal variation in water uptake patterns of three plant species based on stable isotopes in the semi-arid Loess Plateau, Sci. Total Environ., 609, 27–37, 2017.

Wang, J., Lu, N., and Fu, B.: Inter-comparison of stable isotope mixing models for determining plant water source partitioning, Sci. Total Environ. 666, 685–693, 2019b.

Wu, H., Li, J., Li, X., He, B., Liu, J., Jiang, Z., and Zhang, C.: Contrasting response of coexisting plant's water-use patterns to experimental precipitation manipulation in an alpine grassland community of Qinghai Lake watershed, China, PLoS One, 13, e0194242, 2018.

Wu, H., Wu, J., Sakiev, K., Liu, J., Li, J., He, B., Liu, Y., and Shen, B.: Spatial and temporal variability of stable isotopes ($\delta^{18}O$ and $\delta^{2}H$) in surface waters of arid, mountainous Central Asia, Hydrol. Process. 33, 1658–1669, 2019.

Wu, H., Huang, Q., Fu, C., Song, F., Liu, J., Li, J.: Stable isotope signatures of river and lake water from Poyang Lake, China: Implications for river-lake interactions. J. Hydrol. 592, 125619, 2021.

Zhang, P., and Liu, W.: Effect of plant life form on relationship between δD values of leaf wax *n*-alkanes and altitude along Mount Taibai, China, Org. Geochem., 42, 100–107, 2010.

727 Zhao, L., Wang, L., Cernusak, L. A., Liu, X., Xiao, H., Zhou, M., and Zhang, S.:
728 Significant difference in hydrogen isotope composition between xylem and tissue water
729 in *Populus Euphratica*, Plant Cell Environ., 39, 1848–1857, 2016.
730 Zhao, Y., Wang, Y., He, M., Tong, Y., Zhou, J., Guo, X., Liu, J., Zhang, X.: Transference
731 of *Robinia pseudoacacia* water-use patterns from deep to shallow soil layers during the
732 transition period between the dry and rainy seasons in a waterlimited region, For. Ecol.
733 Manag., 457, 117727, 2020.
734 Zhang, H., Cheng, H., Cai, Y., Spötl, C., Sinha, A., Kathayat, G., Li, H.: Effect of
735 precipitation seasonality on annual oxygen isotopic composition in the area of spring
736 persistent rain in southeastern China and its paleoclimatic implication, Clim. Past, 16,
737 211–225, 2020.
738 Zhang, H., Zhang, X., Cai, Y., Sinha, A., Spötl, C., Baker, J., Kathayat, G., Liu, Z., Zhao,
739 J., Jia, X., Du, W., Ning, Y., An, Z., Edwards, R.L., Cheng, H.: A data-model
740 comparison pinpoints Holocene spatiotemporal pattern of East Asian summer monsoon,
741 Quat. Sci. Rev., 261, 106911, 2021.

742

743

744 **Figure captions**

745 **Fig. 1** Sample sites (red dots) and weather stations (open triangles) that distribute along
746 vertical vegetation zones across the Mt. Taibai transect on the Chinese Loess Plateau
747 (a). The meteorological parameters (precipitation, temperature, and RH) vary with
748 stations along elevation transect (b). Mean annul (MAP, MAT, MARH) and montly
749 (MMP, MMT, MMRH) precipitation, temperature, and relative humidity. The
750 subscripts refer to the month. The vertical vegetation distribution was adopted from Liu,

2021.

Fig. 2 Heatmaps of correlations (*r*) between leaf water $\delta^{18}O$ and $\delta^{2}H$ values and potential source water $\delta^{18}O$ and $\delta^{2}H$ values (twig water, soil water, and precipitation $\delta^{18}O$ and $\delta^{2}H$ values; a), and meteorological parameters (e.g., MAP, MMP, MAT, MMT, MARH, MMRH). The hierarchical cluster analysis of the isotopes of leaf water and source water (a), and meteorologica parameters (b). The subscripts (p, soil, twig, leaf) refer to precipitation, soil water, twig water, and leaf water. * Corrected significance at $p < 0.05$; ** corrected significance at $p < 0.01$; *** corrected significance at $p < 0.001$.

Fig. 3 Measured leaf water isotopic composition for $\delta^{18}O$ (a) and $\delta^{2}H$ (c) values against values predicted by the C-G model. Boxplots show no significant differences for $\delta^{18}O$ (b) and $\delta^{2}H$ (d) values between measured and predicted leaf water. The dotted lines show one-to-one lines.

Fig. 4 Correlation of leaf water $\delta^{18}O$ and $\delta^{2}H$ values across months and altitude. Leaf water $\delta^{18}O$ and $\delta^{2}H$ values were the higher in May, intermediate in July, and lower in September, and while within each month, those isotopic values were relatively lower at high altitudes and higher in lower altitudes.

Fig. 5 Variation of monthly mean precipitation $\delta^{18}O$ (a) and $\delta^{2}H$ (b) values at Xi'an station from Global Network of Isotopes in Precipitation (GNIP) and cluster mean of moisture transport routes using HYSPLIT model in May (c), July (d) and September (e), 2020. Background in (c-e) is the average precipitation (mm/day) and 850 hPa wind vectors (arrows, m/s) in May (c), July (d) and September (e) in 1979-2016 AD based on the database of the Global Precipitation Climatology Center (GPCC) (Becker et al., 2011) and the Modern-Era Retrospective analysis for Research and Applications (Rienecker et al., 2011).

Fig. 6 Structural equation model (SEM) of leaf water $\delta^{18}O$ (a) and $\delta^{2}H$ (b) values. The structural equation models considered all plausible pathways. Solid lines indicate significant positive (red) or negative (blue) effects, and dashed lines indicate non-significant effects. Grey lines indicate correlations between two variables. Numbers on the arrow indicate significant standardized path coefficients, proportional to the arrow

width. The coefficients of determination (R^2) represent the proportion of variance explained by the model.

Fig. 7 Schematics of the respective and dual isotopes of $\delta^{18}O$ and $\delta^{2}H$ values from precipitation to leaf water, associated with physical (evaporation at soil profile and transpiration at leaf level) and biochemical processes. The dual isotopes of $\delta^{18}O$ and $\delta^{2}H$ values yield an isotopic water line, the slope of which was lower than the LMWL. The intersected angle varied with hydroclimates, associated with altitude and seasonality.

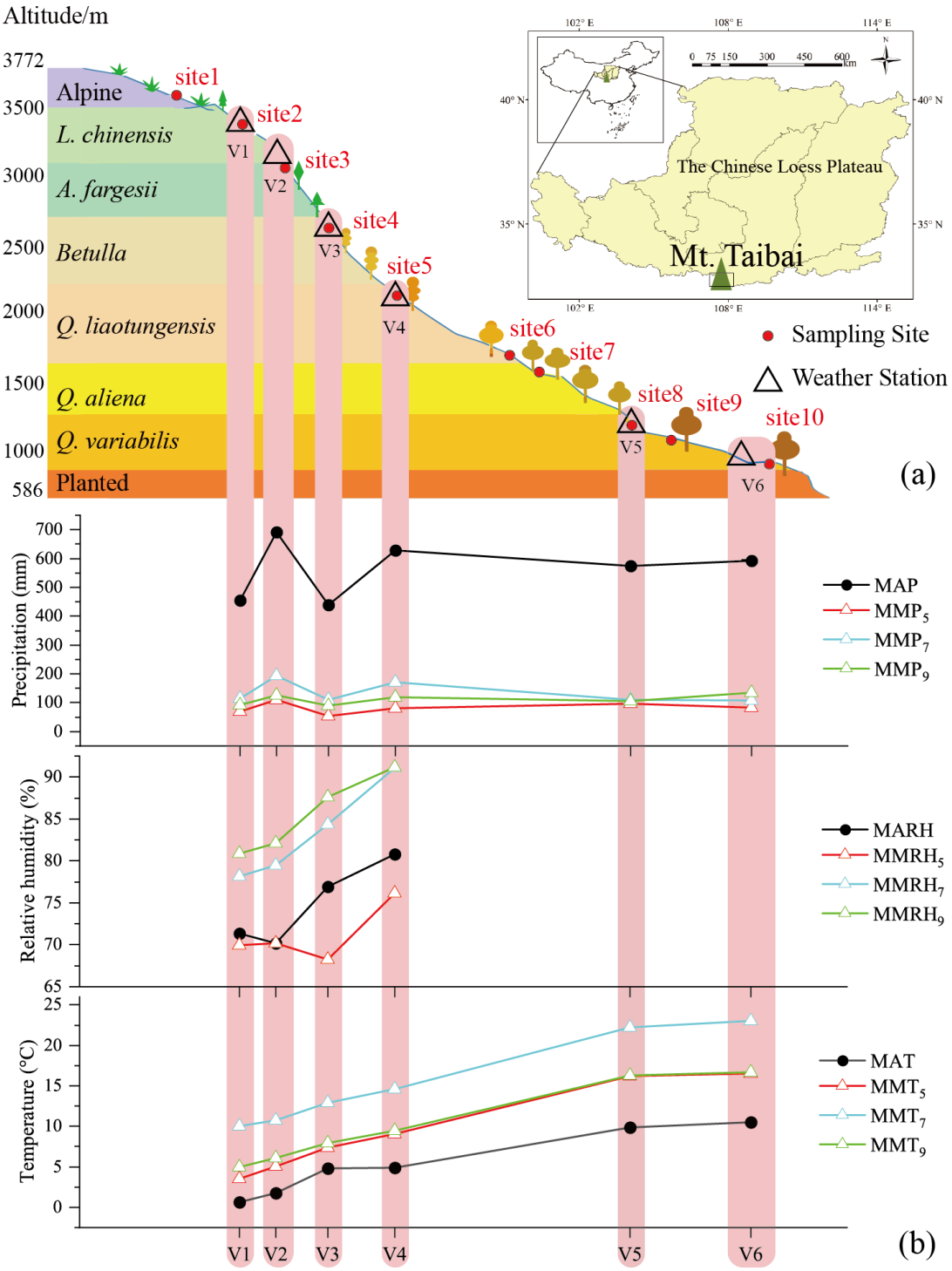
Altitude/m
3772
3500
3000
2500
2000
1500
1000
586
Alpine
L. chinensis
A. fargesii
Betulla
Q. liaotungensis
Q. aliena
Q. variabilis
Planted
site1
site2
site3
site4
site5
site6
site7
site8
site9
site10
V1
V2
V3
V4
V5
V6
102° E
108° E
114° E
40° N
35° N
0 75 150 300 450 600 km
The Chinese Loess Plateau
Mt. Taibai
Sampling Site
Weather Station
(a)
Precipitation (mm)
MAP
MMP5
MMP7
MMP9
Relative humidity (%)
MARH
MMRH5
MMRH7
MMRH9
Temperature (°C)
MAT
MMT5
MMT7
MMT9
(b)

Figure 1

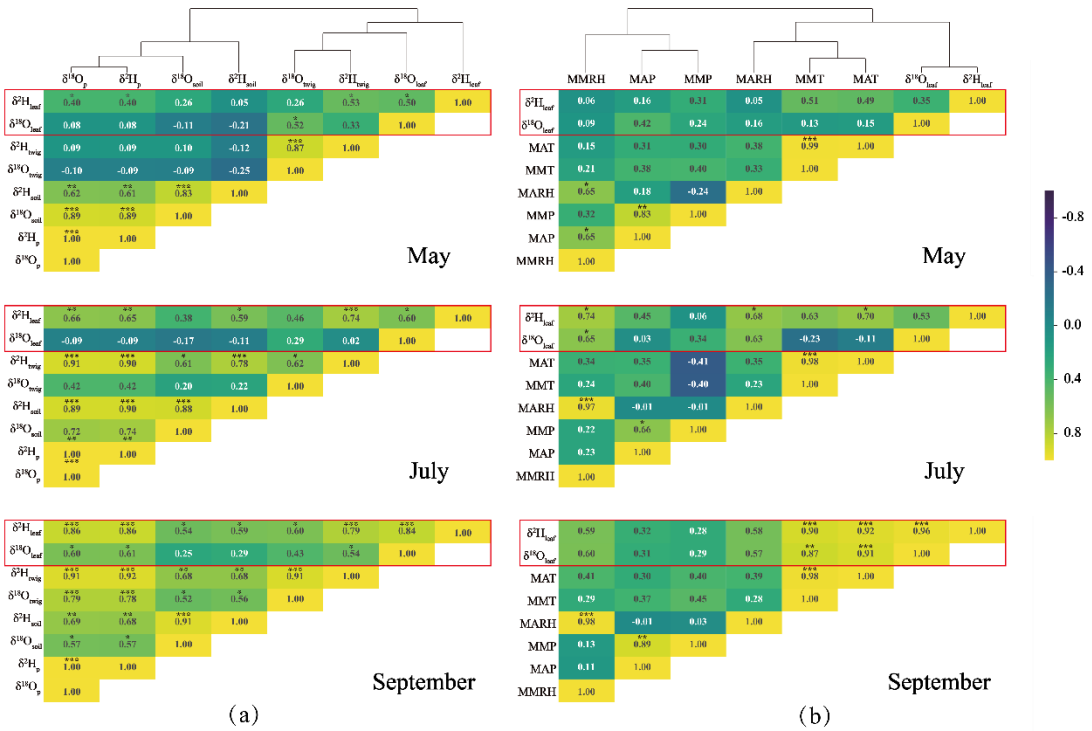

Figure 2

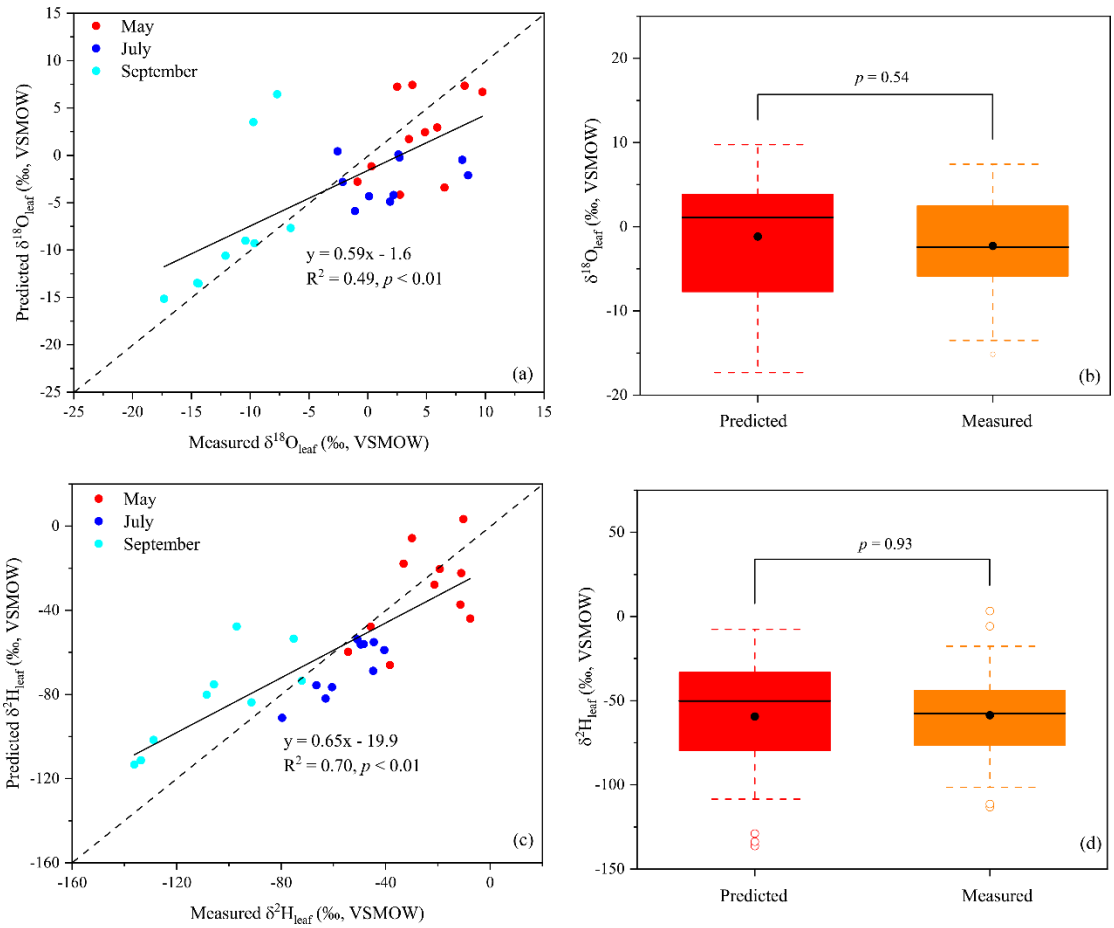

826

827 Figure 3

828

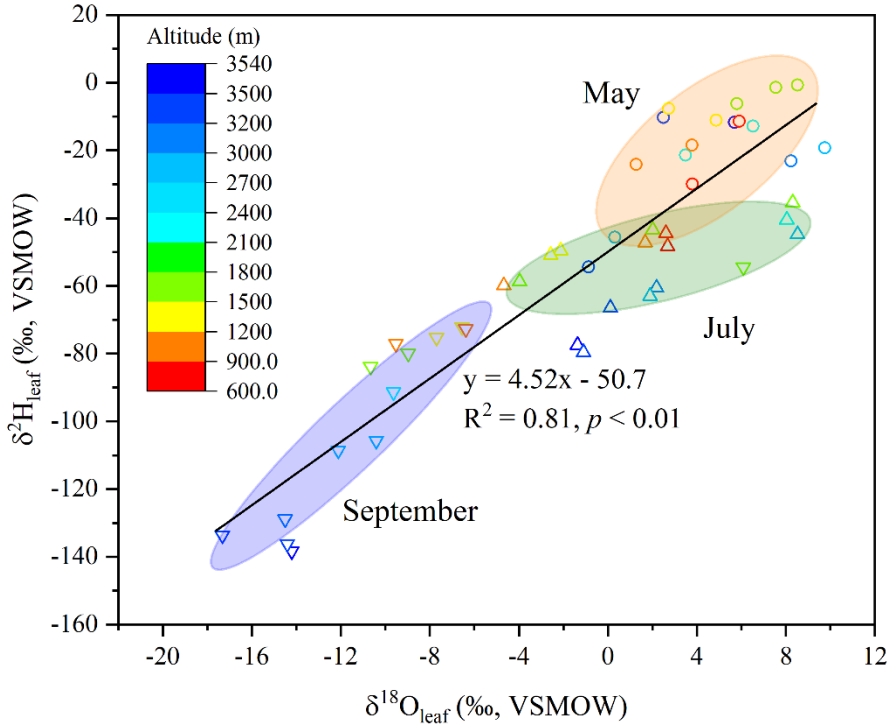

829

830 Figure 4

831

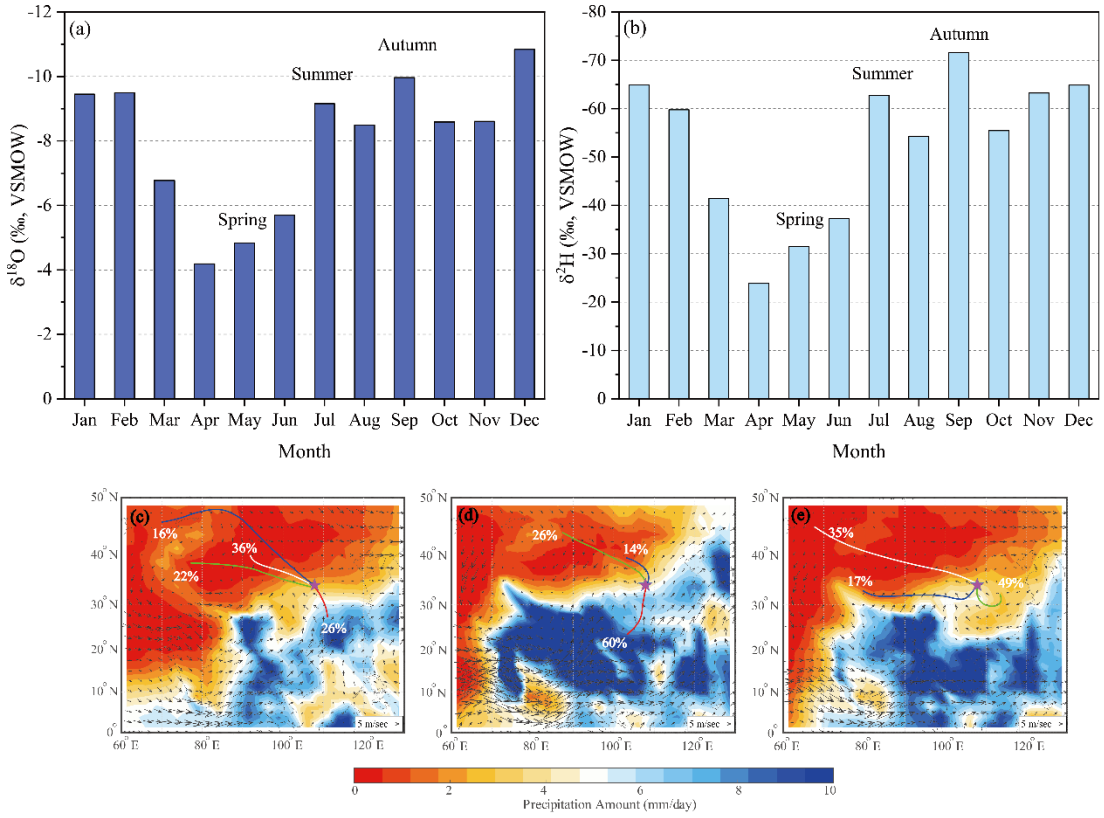

832

833 Figure 5

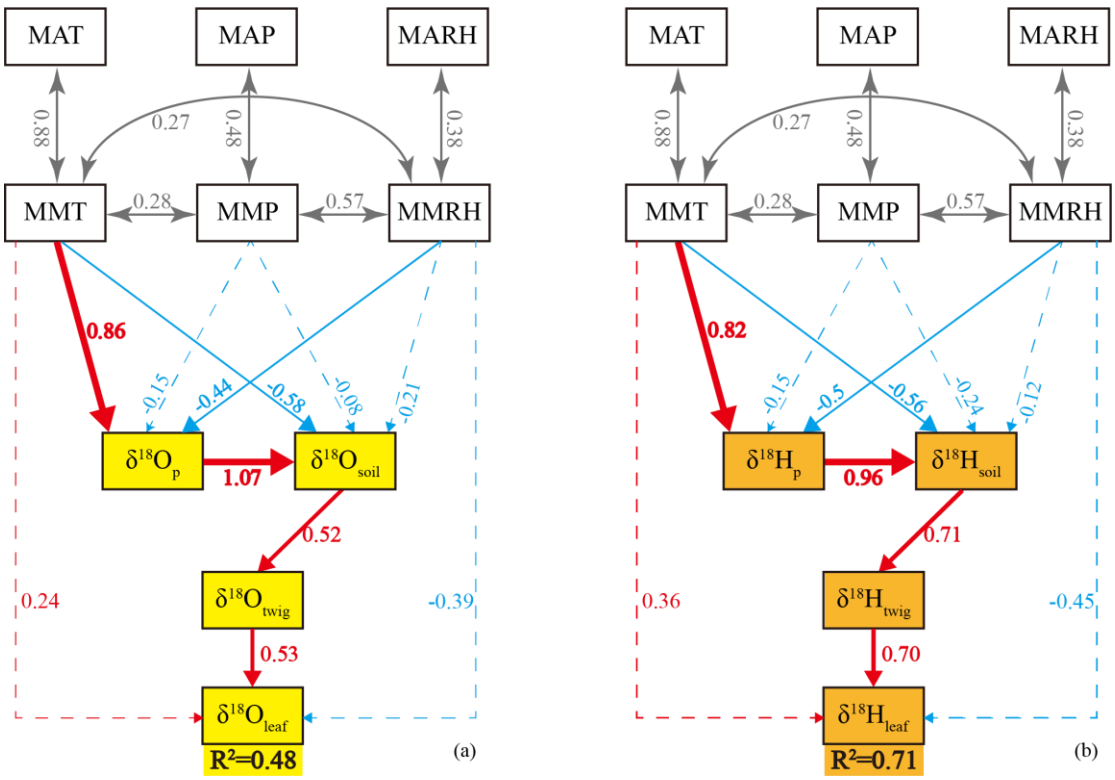

χ^2=15.7, P=0.13
CFI=0.95, GFI=0.89, RMSEA=0.11

χ^2=9.4, P=0.23
CFI=0.99, GFI=0.92, RMSEA=0.01

Figure 6

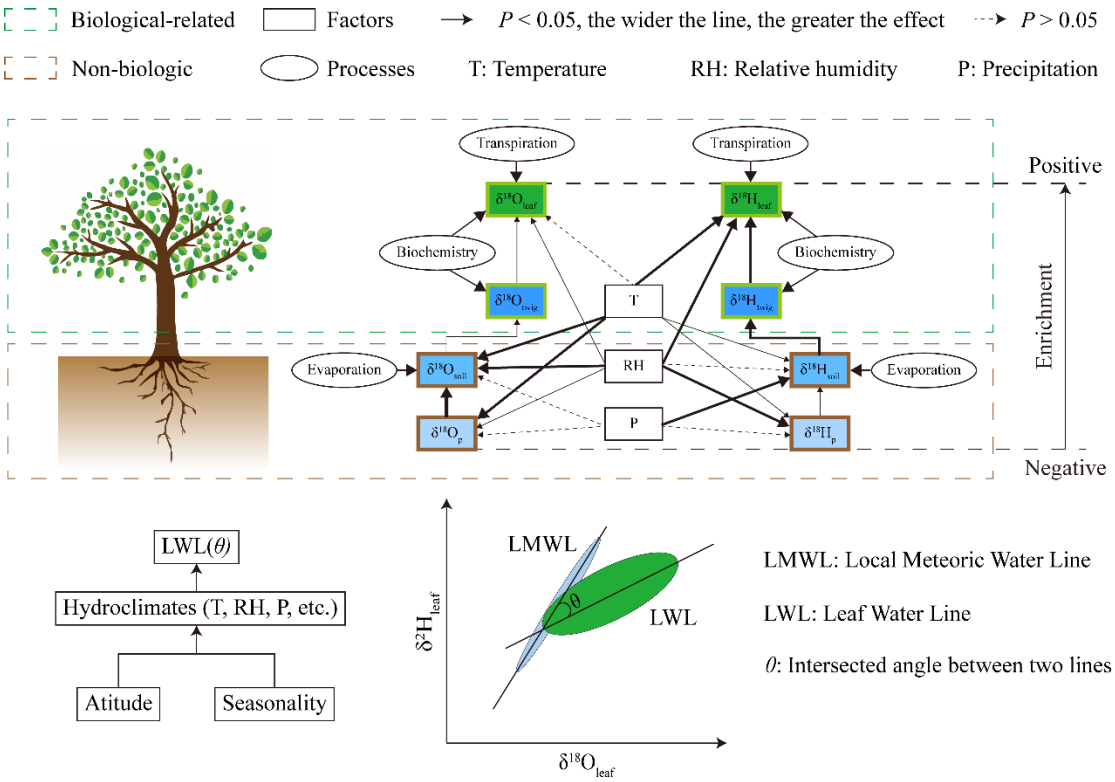

Figure 7